Rare Metal Materials and Engineering
Volume 53, Issue 8, August 2024
Available online at www.rmme.ac.cn

Science Press

Cite this article as: Zhang Min, Ma Chuanchuan, Xue Chun, et al. Effect of Precipitate Phases and Grain Size on Mechanical Properties of Inconel 718 Superalloy After Various Heat Treatments[J]. Rare Metal Materials and Engineering, 2024, 53(08): 2131-2136. DOI: 10.12442/j.issn.1002-185X.20230684.

ARTICLE

Effect of Precipitate Phases and Grain Size on Mechanical Properties of Inconel 718 Superalloy After Various Heat Treatments

Zhang Min, Ma Chuanchuan, Xue Chun, Zhong Wenchang, Gao Bo, Shuai Meirong, Tuo Leifeng, Chu Zhibing

School of Materials Science and Engineering, Taiyuan University of Science and Technology, Taiyuan 030024, China

Abstract: Various heat treatments were conducted on Inconel 718 superalloy, and the resultant microstructures and properties were investigated to analyze the mechanisms of heat treatments. Results show that the type and quantity of precipitate phases and the grain size have different effects on the properties of Inconel 718 superalloy after various heat treatments. The γ'' and γ' phases as well as grain size mainly influence the strength, and the δ phase mainly influences the plasticity. Besides, the precipitation of γ'' and γ' strengthening phases can improve the yield strength. The alloy strength is inversely proportional to mean grain size when the γ'' and γ' phases have similar contents. The plasticity is susceptible to the content and shape of δ phase. A proper amount of δ phase is beneficial to the plasticity, but excessive δ phase degrades plasticity.

Key words: heat treatment; superalloy; precipitates; grain size; mechanical properties

Inconel 718 superalloy, one of the precipitate-strengthened nickel-based superalloys, is widely used in the aero-engine, rocket engine, and nuclear reactor under high-temperature conditions[1–5], owing to its excellent stability in microstructure and mechanical properties at >650 °C. Ref.[6–8] present that the matrix of Inconel 718 superalloy is composed of face-centered cubic (fcc) γ phase, and the precipitate phases mainly consist of body-centered tetragonal γ''-Ni_3Nb phase, fcc γ'-Ni_3(Al, Ti, Nb) phase, and orthorhombic δ-Ni_3Nb phase. Among them, the γ'' and γ' phases are the important strengthening phases[9–11]. In addition, the Laves phase and *M*C carbides also exist in Inconel 718 superalloy. To achieve excellent performance, it is essential to study the precipitates and grain characteristics of the material.

Heat treatment can effectively regulate the precipitates and grain size of the alloy. Ref. [12 – 15] demonstrate that the difference in heat treatments results in different microstructures and grain sizes, which will eventually influence the mechanical properties of alloys. For example, the δ phase affects the strength and plasticity. Huang et al[16] found that the pinning effect results in the δ phase precipitate at the grain boundary during heat treatment. Yadav et al[17] concluded that the coarsened matrix grains can weaken the pinning effect of δ phase and reduce the strength at elevated treatment temperatures. Zhang et al[18] verified that the δ phase degrades the strength but improves the elongation. Ran et al[19] showed that a large quantity of δ phase is beneficial to improve the plasticity. Liu et al[20] suggested that the strength is increased with the increase in size of γ'' and γ' phases. Zhang et al[21] proposed that a certain quantity of γ'' phase can improve the transgranular strength. Caliari et al[22] proposed that increasing the grain size can increase the hardness and creep resistance. Ye et al[23] demonstrated that the fine-grained nickel-based superalloys have excellent ductility and good strength at 550 °C, but they fail to serve at even higher temperatures.

The influence mechanisms about the characteristics and effects of precipitate phases and grains on alloys after various heat treatments are still obscure. Therefore, in this research,

Received date: November 01, 2023
Foundation item: National Natural Science Foundation of China (52175353); Shanxi Province Patent Conversion Special Plan Program (202201001); Shanxi Province Key Research and Development Program (202102150401002)
Corresponding author: Chu Zhibing, Ph. D., Professor, School of Materials Science and Engineering, Taiyuan University of Science and Technology, Taiyuan 030024, P. R. China, E-mail: chuzhibing@tyust.edu.cn

the changes in precipitate phases and grains were analyzed. The potential relationship among heat treatment, microstructure, and properties was discussed. This research provided a theoretical basis to regulate the heat treatment.

1 Experiment

The hot-rolled Inconel 718 superalloy plates were used as the experiment materials, and the chemical composition is shown in Table 1. The plate thickness was 3 mm. All specimens were obtained from the plates by wire cutting. Fig. 1 presents the schematic diagram of tensile specimen. Several rectangular specimens with dimension of 11 mm× 10 mm were prepared for microstructure observation. The tensile specimens were processed into specific shapes according to ASTM E8/E8M-22 standard[24] for the evaluation of tensile properties.

The heat treatment experiments were designed according to the SAE AMS 5383 F standard[25]. In this research, three types of heat treatments were conducted. (1) Double aging (DA): holding at 720 °C for 8 h, furnace cooling to 620 °C at mean cooling rate of 50 °C·s^{-1}, holding at 620 °C for 8 h, and air cooling to room temperature (RT). (2) Standard treatment (ST): solution treatment at 954 °C for 1 h, air cooling to RT, and DA process. (3) High standard treatment (HST): homogenization treatment at 1100 °C for 1 h, air cooling to RT, and ST treatment. During the heat treatments, the heating rates were 5 °C·s^{-1}. The surfaces of the hot-rolled and heat-treated specimens were ground, polished, and chemically etched by Kallings's reagent (5 g $CuCl_2$+100 mL HCl+100 mL CH_3CH_2OH) for 510 s. The microstructure was observed by optical microscope (OM). The mean grain size was calculated by Image Pro Plus software. The phase composition was identified by energy dispersive spectroscopy (EDS). In addition, the tensile experiments of the hot-rolled and heat-treated specimens were conducted by Gleeble 3800 thermal simulator. The deformation temperature was 650 °C, and the strain rate was 0.001 s^{-1}.

2 Results

2.1 Microstructure

Fig. 2a presents the initial microstructure of hot-rolled specimens, which is mainly composed of austenite matrix γ phase, lamellar twins, dispersed carbides, borides, and a small number of γ'', γ', and Laves phases. EDS results show that carbides (MC and $M_{23}C_6$, where M element is mainly Cr element) and borides exist in all specimens. The spherical or block carbides are distributed at the grain boundaries and within the grains. The grains around the banded carbides are smaller than those at other areas owing to the pinning effect. In other words, the banded carbides can prevent the grain elongation during heat treatment. However, the dispersion distribution of carbides may ultimately result in the uneven grain size. According to the grain size distribution in Fig. 2b, the initial mean grain size ($\overline{D}$) is 22.35 μm, and the size of most grains is between 10 and 15 μm.

The treatment temperatures during DA process are 720 and 620 °C, which are both lower than the dissolution temperatures of γ'', γ', and Laves phases. The dissolution and precipitation temperatures of different phases and precipitates are listed in Table 2[26–27]. δ phase is the γ'' phase at stable state. When the aging temperature exceeds 650 °C, the γ'' phase is coarsened and transformed into δ phase. According to Fig. 3a, the content of γ'' and γ' phases in the matrix increases, and the large-sized grains reduce significantly. As shown in Fig. 3b, the size of most grains is 5–10 μm or 10–30 μm based on number frequency or area frequency, respectively. The mean grain size (20.42 μm) slightly decreases. Therefore, the static recrystallization (SRX) occurs during DA process, and the overall uniformity improves.

The temperature of solution treatment (954 °C) is higher

Table 1 Chemical composition of hot-rolled Inconel 718 superalloy (wt%)

C	Si	Mn	P	S	Cr	Ni	Cu	Ti	Nb	B	Co	Al	Ca	Mo	Fe
0.08	0.05	0.03	0.003	0.002	19.00	52.50	0.02	0.90	5.1	0.003	0.02	0.50	0.002	3.01	Bal.

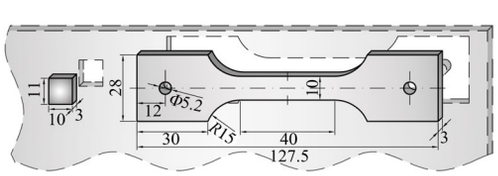

Fig.1 Schematic diagram of tensile specimen

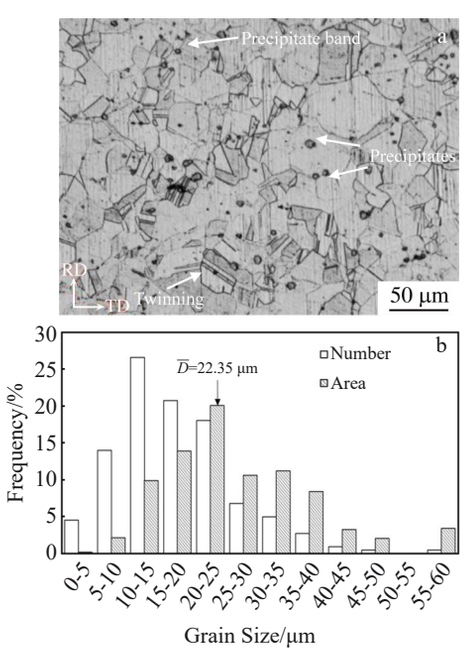

Fig.2 Initial microstructure (a) and grain size distribution (b) of hot-rolled specimen

Table 2 Dissolution and precipitation temperatures of different phases and precipitates in Inconel 718 superalloy (°C)[26–27]

Temperature	γ' phase	γ'' phase	δ phase	Precipitate
Dissolution	843–871	870–930	982–1037	1037
Precipitation	593–816	595–870	780–980	-

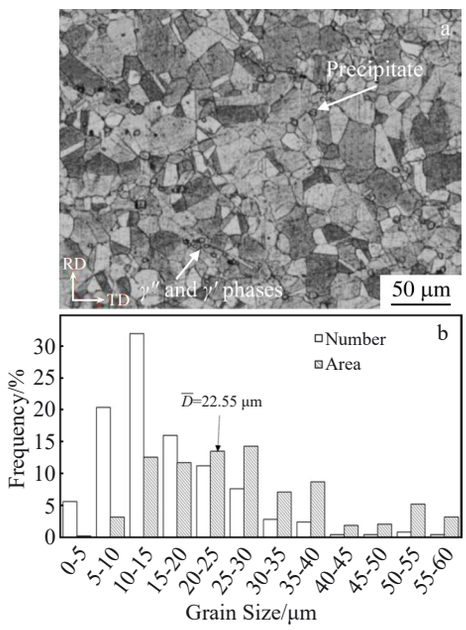

Fig.3 Microstructure (a) and grain size distribution (b) of specimen after DA process

than the dissolution temperatures of γ'' and γ' phases and the precipitation temperature of δ phase. As shown in Fig. 4a, there are a large number of small-sized SRX grains. Most δ phases are in the shape of particles or short rods and precipitated at the grain boundary. Some δ phases are needle-like and often distributed in a linear pattern. According to Fig. 4b, the large-sized grains almost disappear. The sizes of most grains are 5–10 μm. There are small-sized SRX grains near the needle-like δ phase. These phenomena all result from the pinning effect of δ phase.

Based on the microstructure after solution treatment in Fig. 4c, the main alterations after the complete ST process are the precipitation of γ'' and γ' phases and the transformation from γ'' phase into δ phase. The contents of δ phase and SRX grains both increase slightly. According to Fig. 4d, the large-sized grains further reduce. The mean grain sizes after solution treatment and ST process reduce by about 8.64% and 13.86%, respectively. This is because the hindrance against grain boundary movement is enhanced with the increase in δ phase.

Homogenization treatment, as the first stage of HST process, is conducted at 1100 °C. As shown in Fig. 5a, almost all precipitates dissolve, because the temperature exceeds the precipitate dissolution temperature. The grain size increases significantly, compared with that of the initial microstructure. Therefore, both complete recrystallization and grain growth occur. Solution treatment (Fig. 5c) and double aging (Fig. 5e) are the second and third stages of HST process, respectively. The δ phase is precipitated during the solution treatment, and the γ'', γ', and a few δ phases are precipitated during the double aging treatment. The mean grain sizes after the three stages of HST process are 126.21, 113.42, and 103.93 μm, respectively. Therefore, SRX occurs after solid solution and aging treatment. Partial large-sized grains decompose into

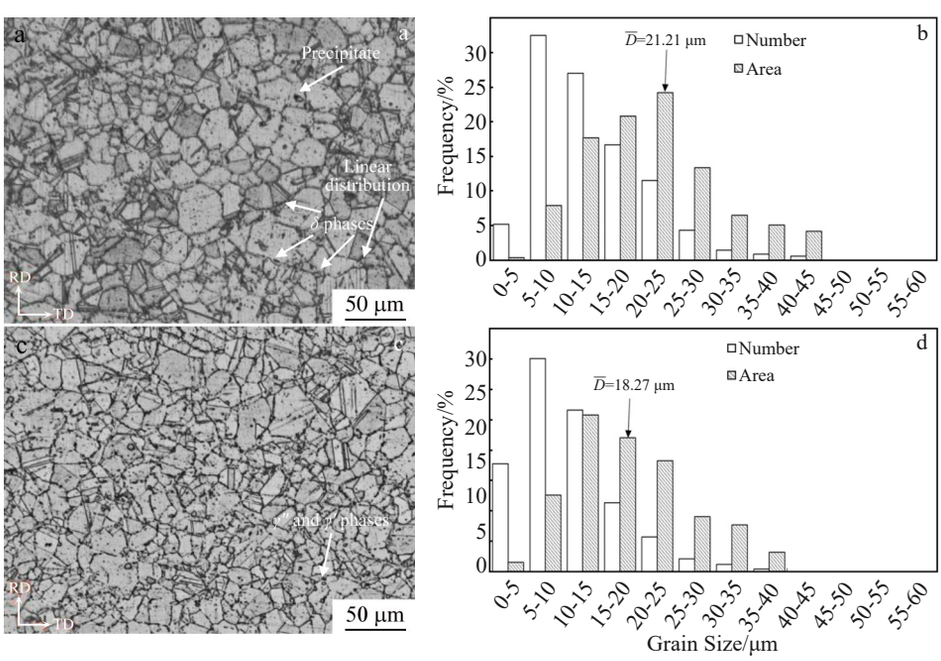

Fig.4 Microstructures (a, c) and grain size distributions (b, d) of specimens after solution treatment (a–b) and double aging treatment (c–d) of ST process

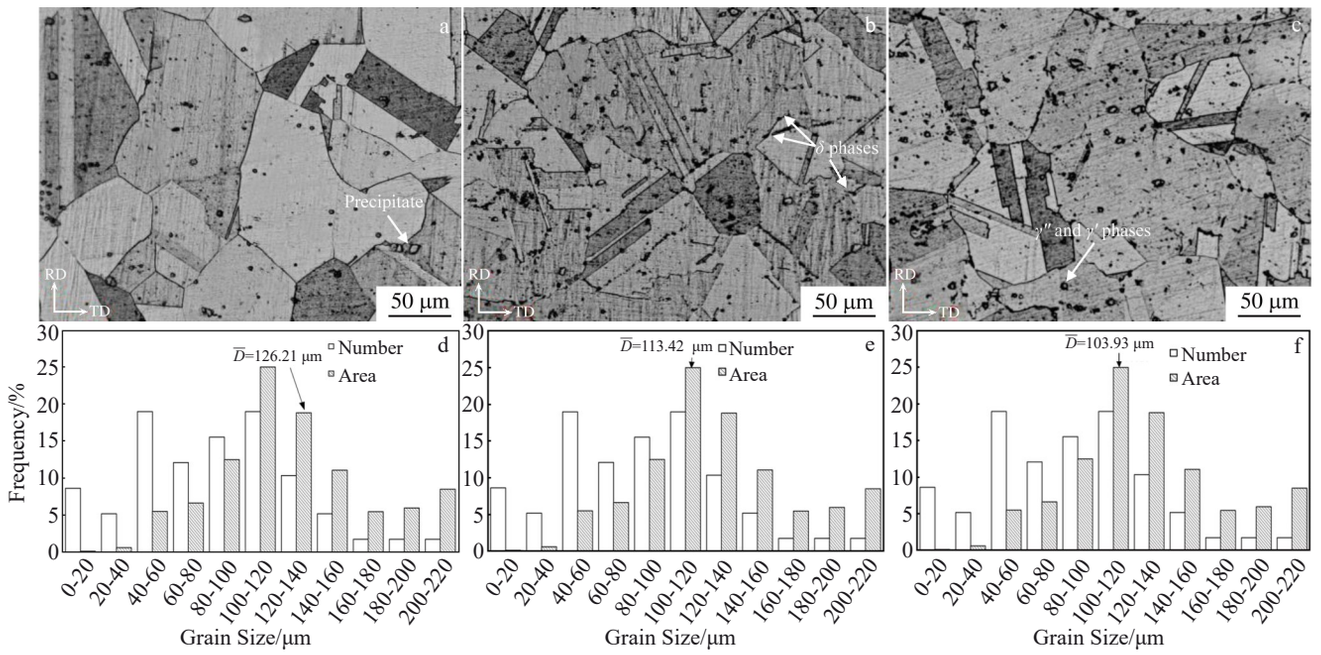

Fig.5 Microstructures (a–c) and grain size distributions (d–f) of specimens after homogenization treatment (a, d), solution treatment (b, e), and double aging treatment (c, f) of HST process

small-sized grains. Consequently, heat treatment has a little effect on the grain refinement.

2.2 Mechanical properties

The tensile stress-strain curves are shown in Fig.6, and the relevant parameters are shown in Table 3. Each tensile stress-strain curve can be divided into six stages: elastic deformation, yield, work hardening, necking, softening (uneven plastic deformation stage), and fracture. The yield strength of heat-treated specimens is more than two times higher than that of the hot-rolled specimen, presenting significant strength increase. The yield strength of specimen after HST process is lower than that after DA and ST processes. The mechanical properties of specimens after DA process is close to those after ST process. The plasticity after any heat treatment degrades. The elongation and area reduction after DA process are better than those after HST and ST processes. The properties of specimens after HST process are similar to those after ST process. In addition, the length of the uneven plastic deformation stage in Fig.6 can reflect the plasticity. This stage length after DA process is longer than that after ST and HST processes, indicating that the plasticity after DA process is optimal. The occurrence of obvious necking after DA process also supports the analysis results.

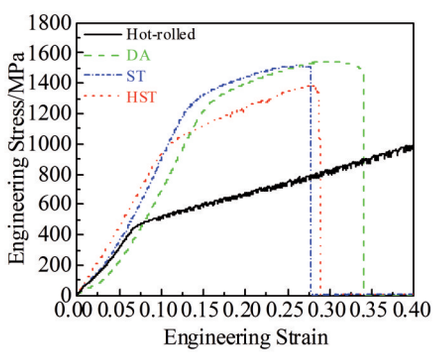

Fig.6 Tensile stress-strain curves of specimens under different conditions

Table 3 Mechanical properties of specimens after different treatments

Treatment	Yield strength/MPa	Tensile strength/MPa	Elongation/%	Area reduction/%
Hot-rolled	523.67	-	-	-
DA	1250.60	1545.65	26.67	27.18
ST	1276.69	1517.07	22.67	19.18
HST	1079.99	1382.19	23.33	20.03

3 Discussion

3.1 Effect of precipitates and grain size on mechanical properties

The heat treatment temperature and holding time can directly affect the precipitates and grain size and finally influence the mechanical properties. The yield strength significantly improves after various heat treatments due to the γ'' and γ' strengthening phases. The yield strength of specimen after DA process is similar to that after ST process, so the δ phase barely has effect on the yield strength. The yield strength after HST process is lower than that after DA and ST processes owing to the dissolution of most Laves phase and the growth of grains. The Laves phase can damage the mechanical properties. The grain refinement can improve the strength of materials[28–30]. Thus, the effect of δ phase on yield strength is the weakest, the co-effect of Laves phase and

grains is in the middle, and the effect of γ'' and γ' phases is the most significant.

The plasticity significantly decreases after various heat treatments because the precipitates hinder the dislocations at the grain boundaries. The plasticity of specimen after DA process is better than that after ST and HST processes, owing to the proper amount of δ phase and less needle-like δ phase. Proper δ phase can balance the grain boundary effect and intragranular strength owing to its pinning effect. However, excessive δ phase destroys the balance and reduces the plasticity. In addition, the needle-like δ phase can hinder the grain boundary migration, which is harmful to the ductility[31–32]. The plasticity of specimen after ST process is similar to that after HST process. Therefore, the co-effect of the Laves phase and grains barely has effect on the plasticity.

3.2 Correlation between grain size and strength

The γ'' and γ' phases and grain size play important roles in strength. Due to the similar contents of γ'' and γ' phases, the strength variation mechanism mainly focuses on the grain size of specimen after various heat treatments. The Hall-Petch relationship[33–37] is widely used to simulate the relationship between flow stress and grain size, as follows:

$$\sigma_{0.2} = \sigma_{hp} + k_{hp} d^m \quad (1)$$

where $\sigma_{0.2}$ is the yield strength; d is the mean grain size; σ_{hp} and k_{hp} are the material parameters; m is the correlation coefficient. The common values of m are −0.5 and −1 in the Hall-Petch relationship.

The $\sigma_{0.2}$-d^m curves with different m values are plotted in Fig.7. Two sets of related parameters can be obtained by linear fitting, as follows:

$$\begin{cases} \sigma_{hp} = 940.07 \\ k_{hp} = 1422.39 \end{cases} \quad m = -0.5 \quad (2)$$

$$\begin{cases} \sigma_{hp} = 1038.05 \\ k_{hp} = 4351.26 \end{cases} \quad m = -1 \quad (3)$$

Substituting the material parameters into Eq. (1), the $\sigma_{0.2}$ value can be obtained, as follows:

$$\sigma_{0.2} = 940.07 + 1422.39 d^{-0.5} \quad m = -0.5 \quad (4)$$

$$\sigma_{0.2} = 1038.05 + 4351.26 d^{-1} \quad m = -1 \quad (5)$$

The root mean squared error (RMSE), average absolute relative error (AARE), and the correlation coefficient (R) can be calculated to evaluate the prediction error of Eq.(4−5), as follows:

$$\mathrm{RMSE} = \sqrt{\frac{\sum_{i=1}^{N} |M_i - A_i|}{N}} \quad (6)$$

$$\mathrm{AARE} = \frac{1}{N} \sum_{i=1}^{N} \left| \frac{M_i - A_i}{A_i} \right| \times 100\% \quad (7)$$

$$R = \frac{\sum_{i=1}^{N} (M_i - \bar{M})(A_i - \bar{A})}{\sum_{i=1}^{N} (M_i - \bar{M})^2 \sum_{i=1}^{N} (A_i - \bar{A})^2} \quad (8)$$

where M_i is the predicted value; A_i is the actual value; N is the number of data; M is the average value of M_i; A is the average value of A_i.

The prediction errors are listed in Table 4. It can be seen that when the m value is −1, RMSE value is small, AARE value is closer to 0, and R value is close to 1. Therefore, the inversely proportional relationship can accurately predict the relationship between yield strength and mean grain size. Due to the good fitting, the strength prediction based on mean grain size is feasible.

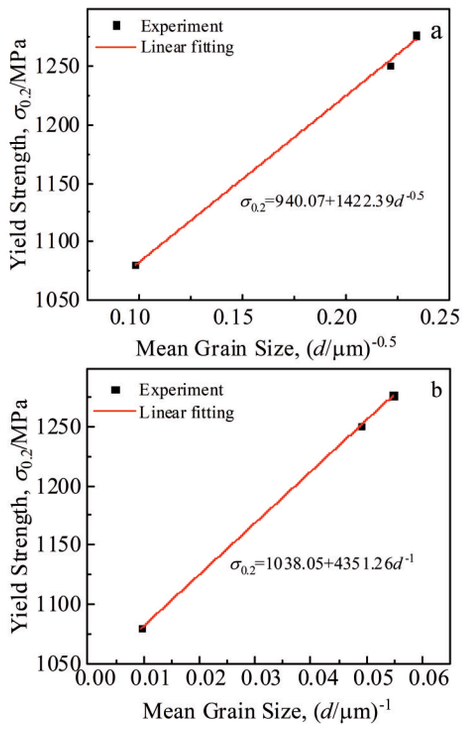

Fig.7 Relationship between yield strength and mean grain size with m=−0.5 (a) and m=−1 (b)

Table 4 Strength prediction errors with different m values

m	RMSE	AARE/%	R
−0.5	2.8268	0.2255	0.9993
−1	0.3622	0.0290	0.9999

4 Conclusions

1) During heat treatment, the temperature and holding time affect the precipitates and grain characteristics. On the one hand, the types and contents of the precipitates are different due to various precipitation and dissolution temperatures. On the other hand, the grain may undergo SRX, complete recrystallization, or even grain growth. However, heat treatment barely has effect on the grain refinement.

2) The types and contents of precipitates as well as grain size affect the mechanical properties. The precipitate of γ'' and γ' strengthening phases and the small-sized grains are beneficial to obtain high strength. The proper δ phase is conducive to high plasticity. Excessive δ phase and needle-liked δ phase can degrade plasticity. The mechanical properties after DA process are optimal due to the fine grains, precipitation of γ'' and γ' phases, and proper δ phase.

3) The effect of δ phase on yield strength is the weakest, the co-effect of Laves phase and grains is in the middle, and the

effect of γ'' and γ' phases is the most significant. Besides, the strength is inversely proportional to the mean grain size according to the Hall-Petch relationship.

4) The content and shape of the δ phase are primary influence factors for the plasticity. The Laves phase and grains barely have effect on the plasticity.

References

1 Xiao G F, Xia Q X, Zhang Y L *et al*. *International Journal of Advanced Manufacturing Technology*[J], 2021, 117: 199
2 Chen J T, Lu J X, Cai W *et al*. *International Journal of Plasticity*[J], 2023, 163: 103554
3 Han D W, Yu L X, Liu F *et al*. *Acta Metallurgica Sinica* (*English Letters*)[J], 2018, 31(11): 1224
4 Liu T, Cheng X N, Luo R *et al*. *Materials Science & Engineering A*[J], 2021, 819: 141533
5 Wang J G, Liu D, Ding X *et al*. *Crystals*[J], 2020, 10(4): 303
6 Wei Bo. *Research on Heat-Assisted Incremental Bending Forming Technology of Large Curvature Metal Plates*[D]. Guangzhou: South China University of Technology, 2021 (in Chinese)
7 Zheng Xin, Shi Yuying, Chen Yubao. *Heat Treatment of Metals*[J], 2018, 43(6): 162 (in Chinese)
8 Jiang S Y, Sun D, Zhang Y Q *et al*. *Metals*[J], 2018, 8(4): 217
9 Xia T, Xie Y H, Yang C *et al*. *Materials Characterization*[J], 2018, 145: 362
10 Dinh B N N, Bäker M. *Metallurgical and Materials Transactions A*[J], 2023, 54A: 1857
11 Du J H, Lv X D, Deng Q. *Rare Metal Materials and Engineering*[J], 2014, 43(8): 1830
12 Ahmad N, Ghiaasiaanb R, Gradl P R *et al*. *Materials Science & Engineering A*[J], 2022, 849: 143528
13 Ran R, Wang Y, Zhang Y X *et al*. *Journal of Materials Research and Technology*[J], 2022, 20: 1216
14 Yu X F, Hu C Y, Liu H X *et al*. *Journal of Materials Science*[J], 2022, 57: 7965
15 Liu Lirong, Jin Tao, Zhao Nairen *et al*. *Rare Metal Materials and Engineering*[J], 2006, 35(5): 711 (in Chinese)
16 Huang R S, Sun Y A, Xing L L *et al*. *Materials Science & Engineering A*[J], 2020, 774: 138913
17 Yadav P C, Sahu S, Subramaniam A *et al*. *Materials Science & Engineering A*[J], 2018, 715: 295
18 Zhang C, Yu L M, Wang H *et al*. *Materials*[J], 2019, 12(13): 2096
19 Ran R, Wang Y, Zhang Y X *et al*. *Journal of Alloys and Compounds*[J], 2022, 927: 166820
20 Liu A Q, Zhao F, Huang W S *et al*. *Crystals*[J], 2023, 13(6): 964
21 Zhang Y C, Yang L, Chen T Y *et al*. *Optics and Laser Technology*[J], 2017, 97: 172
22 Caliari F R, Candioto K C G, Couto A A *et al*. *Journal of Materials Engineering and Performance*[J], 2016, 25: 2307
23 Ye X J, Yang B B, Liu J T *et al*. *Materials*[J], 2022, 15(13): 4524
24 ASTM international Committee. *ASTM Standard*, E8/E8M-22[S], 2022
25 AMS Committee. *US Patent*, AMS5383[P], 2018
26 Zhu Qiang. *Mesoscopic Plastic Deformation Mechanism of GH4169 Nickel-Based Superalloy Thin Sheet*[D]. Harbin: Harbin Institute of Technology, 2020 (in Chinese)
27 Gai Y C, Zhang R, Yang J X *et al*. *Materials Science & Engineering A*[J], 2022, 842: 143079
28 Zhou X, Li X Y, Lu K. *Science*[J], 2018, 360(6388): 526
29 Zhang Taiquan, Long Benfu, Lin Gaoan. *Materials China*[J], 2022, 41(6): 466 (in Chinese)
30 Li Ting, Du Yu, Qu Lei *et al*. *Titanium Industry Progress*[J], 2022, 39(5) 22 (in Chinese)
31 Sun W, Chu X, Huang J B *et al*. *Coatings*[J], 2022, 12(3): 347
32 Zhang H J, Li C, Guo Q Y *et al*. *Materials Science & Engineering A*[J], 2018, 722: 136
33 Liu B B, Han J Q, Zhao R *et al*. *High Temperature Material Processes*[J], 2016, 35(10): 989
34 Hansen N, Ralph B. *Acta Metallurgica*[J], 1982, 30(2): 411
35 Haouala S, Segurado J, Lorca J. *Acta Materialia*[J], 2018, 148: 72
36 Hall E O. *Proceedings of the Physical Society, Section B*[J], 1951, 64(9): 747
37 Petch N J. *Journal of the Iron and Steel Institute*[J], 1953, 174(19): 25

不同热处理下析出相和晶粒尺寸对Incone1 718高温合金力学性能的影响

张　旻，马川川，薛　春，钟文昌，高　波，帅美荣，拓雷锋，楚志兵

(太原科技大学 材料科学与工程学院，山西 太原 030024)

摘　要：采用不同热处理工艺对Inconel 718高温合金进行了组织观察和性能研究以分析热处理机理。结果表明，析出相的类型和数量以及晶粒尺寸对Inconel 718高温合金热处理试样的性能有不同的影响。γ''相和γ'相以及晶粒尺寸主要影响强度，δ相主要影响塑性。此外，γ''和γ'强化相的析出可以提高屈服强度。合金中γ''和γ'相含量相近时，强度与平均晶粒尺寸成反比。塑性易受δ相含量和形状的影响。适量的δ相对塑性有益，但过量的δ相会使塑性降低。

关键词：热处理；高温合金；析出相；晶粒尺寸；力学性能

作者简介：张　旻，女，1998年生，博士生，太原科技大学材料科学与工程学院，山西 太原 030024，E-mail：B202214110025@stu.tyust.edu.cn